

# Chaotic communication in radio-over-fiber transmission based on optoelectronic feedback semiconductor lasers

Fan-Yi Lin\* and Meng-Chiao Tsai

*Institute of Photonics Technologies, Department of Electrical Engineering,  
National Tsing Hua University,  
Hsinchu 300, Taiwan  
[fylin@ee.nthu.edu.tw](mailto:fylin@ee.nthu.edu.tw)*

**Abstract:** Performance of chaotic communication in radio-over-fiber (ROF) transmission based on optoelectronic feedback semiconductor lasers is studied numerically. The chaotic carrier is generated by optoelectronic feedback semiconductor lasers, where chaotic communication is realized by synchronizing a receiver laser with a transmitter laser. Transmission quality of different message encoding schemes, including additive chaos modulation (ACM) and on-off shift keying (OOK), are investigated and compared. In this study, the dispersion and nonlinearity effects in the fiber transmission module and the amplified spontaneous emission noise from the optical amplifiers are considered. In the wireless channel, effects of additive white Gaussian noise, multipath, and path loss are included. To quantitatively study the performance of this chaotic communication system in the ROF transmission, bit-error-rates (BER) of different transmission lengths, message bit-rates, and signal-to-noise ratios are studied. The optimal launched power and message strength that minimize the BER while assuring effective communication security are discussed. While the ACM scheme is shown to perform better in a fiber only configuration, the OOK scheme shows better immunity to the random effects and waveform distortions presented in the wireless channel.

© 2007 Optical Society of America

**OCIS codes:** (140.5960) Semiconductor lasers, (060.2330) fiber optics communications.

---

## References and links

1. F. Y. Lin and J. M. Liu, "Nonlinear dynamical characteristics of an optically injected semiconductor laser subject to optoelectronic feedback," *Opt. Commun.* **221**, 173–180 (2003).
2. S. K. Hwang and J. M. Liu, "Dynamical characteristics of an optically injected semiconductor laser," *Opt. Commun.* **183**, 173–180 (2003).
3. T. B. Simpson and J. M. Liu, A. Gavrielides, V. Kovanis, P. M. Alsing, "Period-doubling route to chaos in a semiconductor laser subject to optical injection," *Appl. Phys. Lett.* **64**, 3539–3541 (1994).
4. T. Mukai and K. Otsuka, "New route to optical chaos: successive-subharmonic-oscillation cascade in a semiconductor laser coupled to an external cavity," *Phys. Rev. Lett.* **55**, 1711–1714 (1985).
5. J. Mork, B. Tromborg, and J. Mark, "Chaos in semiconductor lasers with optical feedback: theory and experiment," *IEEE J. Quantum Electron.* **28**, 93–108 (1992).
6. F. Y. Lin and J. M. Liu, "Nonlinear dynamics of a semiconductor laser with delayed negative optoelectronic feedback," *IEEE J. Quantum Electron.* **39**, 562–568 (2003).

7. S. Tang and J. M. Liu, "Chaotic pulsing and quasi-periodic route to chaos in a semiconductor laser with delayed opto-electronic feedback," *IEEE J. Quantum Electron.* **37**, 329–336 (2001).
8. F. Y. Lin and J. M. Liu, "Harmonic frequency locking in a semiconductor laser with delayed negative optoelectronic feedback," *Appl. Phys. Lett.* **81**, 3128–3120 (2002).
9. N. Gastaud, S. Poinsot, L. Larger, J. M. Merolla, M. Hanna, J. P. Goedgebuer and F. Malassenet, "Electro-optical chaos for multi-10 Gbit/s optical transmissions" *Electron. Lett.* **40**, (2004).
10. J. M. Liu, H. F. Chen, and S. Tang, "Synchronized chaotic optical communications at high bit rates," *IEEE J. Quantum Electron.* **38**, 1184–1196 (2002).
11. J. Ohtsubo, "Chaos synchronization and chaotic signal masking in semiconductor lasers with optical feedback," *IEEE J. Quantum Electron.* **38**, 1141–1154 (2002).
12. Y. Liu, H. F. Chen, J. M. Liu, P. Davis, and T. Aida, "Communication using synchronization of optical-feedback-induced chaos in semiconductor lasers," *IEEE Trans. Circuits Syst. I* **48**, 1484–1490 (2001).
13. D. Kanakidis, A. Argyris, and D. Syvridis, "Performance characterization of high-bit-rate optical chaotic communication systems in a back-to-back configuration," *J. of Lightwave Technol.* **21**, 750–758 (2003).
14. A. Argyris, D. Syvridis, L. Larger, V. Annovazzi-Lodi, P. Colet, I. Fischer, J. Garcia-Ojalvo, C. R. Mirasso, L. Pesquera, and K. A. Shore, "Chaos-based communications at high bit rates using commercial fibre-optic links," *Nature* **438**, 343–346 (2005).
15. D. Kanakidis, A. Bogris, A. Argyris, and D. Syvridis, "Numerical investigation of fiber transmission of a chaotic encrypted message using dispersion compensation schemes," *J. of Lightwave Technol.* **22**, 2256–2263 (2004).
16. S. Tang and J. M. Liu, "Chaos synchronization in semiconductor lasers with optoelectronic feedback," *IEEE J. Quantum Electron.* **39**, 708–715 (2003).
17. H. D. I. Abarbanel, M. B. Kennel, L. Illing, S. Tang, H. F. Chen, and J. M. Liu, "Synchronization and communication using semiconductor lasers with optoelectronic feedback," *IEEE J. Quantum Electron.* **37**, 1301–1311 (2001).
18. J. M. Liu and T. B. Simpson, "Four-wave mixing and optical modulation in a semiconductor laser," *IEEE J. Quantum Electron.* **30**, 957–965 (1994).
19. V. Sinkin, R. Holzlohner, J. Zweck, and C. R. Menyuk, "Optimization of the split-step Fourier method in modeling optical-fiber communication systems," *J. Lightwave Technol.* **21**, 61–68 (2003).
20. L. Wei and C. Schlegel, "Synchronization requirements for multi-user OFDM on satellitemobile and two-path Rayleigh fading channels," *IEEE Trans. on Commun.* **43**, 887–895 (1995).

## 1. Introduction

Optical chaotic communication has been studied extensively in recent years. In general, the chaotic carriers can be generated by semiconductor lasers through optical injection [1, 2, 3], optical feedback [4, 5], optoelectronic feedback [6, 7, 8], and electro-optic feedback [9]. The message recovery is done by synchronizing a receiver laser to a transmitter laser [10]. While chaotic communications have been proven feasible in a back-to-back configuration [10, 11, 12, 13], studies with scenarios as in the practical communication environments have to be considered.

To extend the distance of transmission, chaotic communication with transmission through optical fiber based on an electro-optics scheme has been studied [14]. Performance of chaotic communication including transmission in dispersion shifted fibers based on optical feedback system is characterized numerically [15]. To further extend the transmission into a wireless channel, we study the performance of chaotic communication system in a radio-over-fiber (ROF) scenario based on an OEF scheme. Compared to the OI and OF systems that require stringent optical phase synchronization, the OEF scheme can be synchronized easily and does not require expensive high-speed modulator as needed in an EO scheme.

In this paper, we first consider the effect of the fiber module in a chaotic communication system based on optoelectronic feedback laser. Furthermore, the random influences and additional noises from the wireless channel are added and discussed. This radio-over-fiber configuration not only extends the transmission distance, but also provides the possible mobility and portability for secured communications.

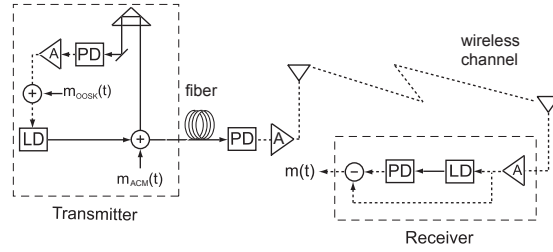


Fig. 1. Schematic setup of the chaotic communication in ROF system based on optoelectronic feedback semiconductor lasers. Dashed and solid lines indicate electronic and optic paths, respectively.

## 2. Simulation model

### 2.1. Transmitter and receiver lasers

Figure 1 shows the schematic setup of the chaotic communication in radio-over-fiber (ROF) system based on optoelectronic feedback semiconductor lasers. In the transmitter, the laser output is converted into electric current through a photodetector and fed back to the laser through the bias current. The nonlinear dynamics of the transmitter laser can be controlled by varying the operational parameters, namely the feedback strength and the delay time. Message recovery is done by synchronizing the receiver laser with the transmitter laser in an open-loop configuration, in which the receiver laser has similar intrinsic parameters with the transmitter laser [16, 17]. The transmitter and the receiver lasers are simulated using the model described in [1, 6] with the following normalized dimensionless rate equations:

$$\frac{da_{t,r}}{dt} = \frac{1}{2} \left[ \frac{\gamma_c \gamma_n}{\gamma_s \tilde{J}_{t,r}} \tilde{n}_{t,r} - \gamma_p (2a_{t,r} + a_{t,r}^2) \right] (1 + a_{t,r}) \quad (1)$$

$$\frac{d\phi_{t,r}}{dt} = -\frac{b}{2} \left[ \frac{\gamma_c \gamma_n}{\gamma_s \tilde{J}_{t,r}} \tilde{n}_{t,r} - \gamma_p (2a_{t,r} + a_{t,r}^2) \right] \quad (2)$$

$$\begin{aligned} \frac{d\tilde{n}_{t,r}}{dt} = & -\gamma_s \tilde{n}_{t,r} - \gamma_n (1 + a_{t,r})^2 \tilde{n}_{t,r} - \gamma_s \tilde{J} (2a_{t,r} + a_{t,r}^2) + \frac{\gamma_s \gamma_p}{\gamma_c} \tilde{J}_{t,r} (2a_{t,r} + a_{t,r}^2) (1 + a_{t,r})^2 \\ & + \xi_{t,r} \gamma_s (\tilde{J}_{t,r} + 1) (1 + 2a_t(t - \tau_{t,r}) + a_t(t - \tau_{t,r})^2) \end{aligned} \quad (3)$$

Here,  $a$  is the normalized field,  $\phi$  is the optical phase,  $\tilde{n}$  is the normalized carrier density,  $\gamma_c$ ,  $\gamma_s$ ,  $\gamma_n$ , and  $\gamma_p$  are the cavity decay rate, spontaneous carrier decay rate, differential carrier relaxation rate and the nonlinear carrier relaxation rate, respectively,  $b$  is the linewidth enhancement factor, and  $\tilde{J}$  is the normalized dimensionless injection current parameter. The subscript  $r$  and  $t$  refer to the transmitter and the receiver lasers respectively. For the transmitter laser, the output is fed back with a feedback strength  $\xi_t$  and a delay time  $\tau_t$ , while the receiver laser is injected with a coupling strength  $\xi_r$  and a transmission propagation time  $\tau_r$ , respectively. In our simulation, the following experimentally measured intrinsic dynamical parameters of a high-speed semiconductor laser [18] are used for both the transmitter and the receiver lasers:  $\gamma_c = 2.4 \times 10^{11} s^{-1}$ ,  $\gamma_s = 1.458 \times 10^9 s^{-1}$ ,  $\gamma_n = 3\tilde{J} \times 10^9 s^{-1}$ ,  $\gamma_p = 3.6\tilde{J} \times 10^9 s^{-1}$ , and  $b = 4$ . The lasers are both biased at a value of  $\tilde{J} = 1/3$ , while the feedback and coupling strengths  $\xi_t$  and  $\xi_r$  are both set to a level of 0.1. With this coupling strength, the receiver laser is operated in a linear operation regime that it is identically synchronized to the transmitter laser [16, 17]. The relaxation oscillation frequency of the laser is  $f_r = (\gamma_c \gamma_n + \gamma_s \gamma_p)^{1/2} / 2\pi$ , which is about 2.49 GHz with the parameters used in this simulation. Second-order Runge-Kutta method is used to

solve these coupled rate equations.

## 2.2. ACM and OOSK message encoding schemes

Two message encoding schemes, including additive chaotic modulation (ACM) and on-off shift keying (OOSK), are considered and compared in this study. As shown in Fig. 1, for the ACM scheme, the message is modulated onto the chaotic carrier and is transmitted to the receiver and fed back to the transmitter simultaneously. For the OOSK scheme, on the other hand, the message is encoded by modulating the bias current of the transmitter laser so that the laser is switching, or shifting, back and forth between two different dynamic states. In the ACM scheme, message recovery is done by synchronizing the receiver laser with the transmitter laser and then subtract the reproduced chaotic waveform from the channel signal, while in the OOSK scheme, the decoding is realized by calculating the synchronization error between the two lasers to identify if the transmitter laser is in an ON (bit 1) or an OFF (bit 0) state.

## 3. Fiber transmission module

### 3.1. Description of the fiber transmission module

In this ROF chaotic communication system, the dispersion and nonlinearity effects in the fiber module is described by the nonlinear Schrödinger equation (NLSE) [15]:

$$j \frac{\partial A}{\partial z} = -\frac{j}{2} \alpha A - \gamma |A|^2 A + \frac{1}{2} \beta_2 \frac{\partial^2 A}{\partial T^2} + \frac{1}{6} \beta_3 \frac{\partial^3 A}{\partial T^3} \quad (4)$$

, where  $A$  is the complex intracavity laser field amplitude,  $z$  is the propagation distance,  $T$  is the time measured in a reference frame moving at group velocity,  $\alpha$  is the fiber attenuation coefficient,  $\gamma$  is the nonlinear coefficient, and  $\beta_2$  and  $\beta_3$  are the second-order and third-order chromatic dispersions. The split-step Fourier method (SSFM) [19] is used to solve the nonlinear Schrödinger equation in this study. It was numerically observed that chromatic dispersion in the fiber distorts the transmitted waveform and therefore increases the synchronization error significantly [15]. To obtain satisfactory communication performance, dispersion-shifted fiber in a dispersion compensation map is considered in this study. The fiber parameters used are  $\alpha = 0.21$  dB/km,  $\beta_2 = 0.1$  ps<sup>2</sup>/km,  $\beta_3 = 0.1$  ps<sup>3</sup>/km, and  $\gamma = 1.5$  W<sup>-1</sup>km<sup>-1</sup>, respectively.

The fiber loss is compensated by amplifying the optical signal with optical amplifiers. These amplifiers bring the optical power of the signal back to the original launched power level, but simultaneously introduce additional amplified spontaneous emission (ASE) noise. The ASE noise is modelled by an additive Gaussian noise with variance  $\sigma^2 = n_{sp} h f (G - 1) \Delta f$ , where  $G$  is the amplifier gain to compensate transmission loss,  $n_{sp}$  accounts for incomplete population inversion,  $h$  is Plank's constant,  $f$  is the signal carrier frequency and  $\Delta f$  is the bandwidth occupied by each discrete Fourier spectrum component. In our simulation,  $n_{sp}$  is set to 2, or noise figure of 6 equivalently.

### 3.2. Results with fiber transmission module

To optimize the performance while not compromising the security in communication, both the initial power launched into the fiber and the strengths of the modulated messages are carefully investigated and are presented in Fig. 2. Figure 2(a) shows the BERs of the ACM and OOSK schemes after propagating 50 km in the fiber with different initial launched powers. The launched power is normalized to 4.5 mW (0 dB), which is the laser output power at free-running condition. As can be seen, if the launched power is too high, severe distortions caused by the nonlinear effect of the fiber degrade the decoding performance and result in a high BER. Best BERs are found at normalized launched powers of -6 and -8 dB for the ACM and the

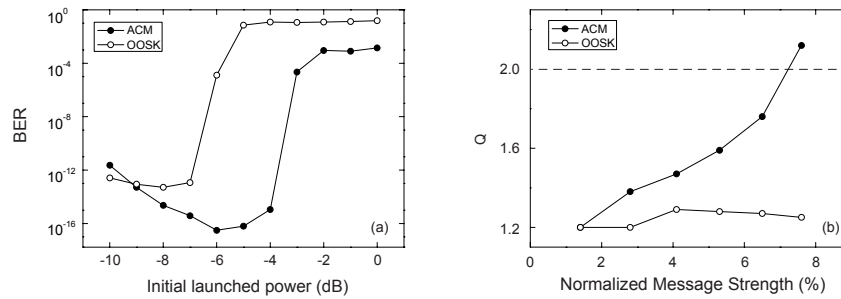


Fig. 2. (a) BER of different initial launched powers and (b) Q of different normalized message strengths for the ACM and OOSK schemes, respectively. The length of the fiber is 50 km.

OOSK schemes, respectively. For a power that is lower than these optimal launched powers, system performance degrades again due to the increased ASE noise from the necessary optical amplifiers.

A large modulation depth of the message in general provides a better SNR, thus better decoding performance. However, to ensure the communication security, the message strength has to be kept under a certain value so that the message cannot be recovered by an intruder without synchronizing to the transmitter laser but simply filtering the channel signal. The benchmark of this critical value can be defined as when the filtered signal has a Q-factor lower than 2, where the eye in the eye-diagram is hardly opened. Figure 2(b) shows the Q of the filtered channel signal of both the ACM and OOSK schemes with different message strengths. For the ACM scheme, the normalized message strength is defined as the ratio between the message power and the output power of the laser. For the OOSK scheme, the normalized message strength is defined as the ratio between the modulation current to the DC biased current. As can be seen, with a normalized message strength of less than 7 percents, the Q for both schemes fall below the benchmark of 2. In this study, the message strengths of the ACM and the OOSK schemes are chosen to be at 1.4 and 4.1 percents, respectively, which the corresponding Q of the filtered signals are both well below the benchmark so that the security is ensured.

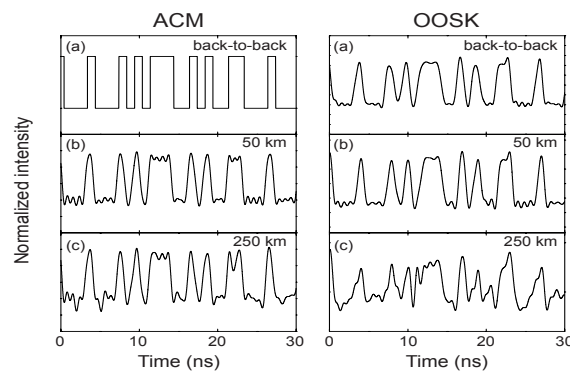


Fig. 3. Decoded messages of the ACM and OOSK schemes after propagating over fiber with lengths of (a) 0 (back-to-back), (b) 50 km, and (c) 250 km, respectively.

With the optimal launched powers and message strengths chosen, the decoded messages of the ACM and the OOSK schemes with a message bit-rate of 1 Gbps are plotted in Fig. 3. Figures 3(a)-(c) show the decoded messages after propagating over fiber with lengths of 0 (back-to-back), 50 km, and 250 km, respectively. For the back-to-back case shown in Fig. 3(a), the ACM scheme shows perfect synchronization and the encoded message is fully recovered. This is because the encoding message adds equally to the bias currents of the transmitter and the receiver lasers, which makes them identical to each other and therefore have a perfect synchronization. For the OOSK scheme, on the contrary, the message is encoded and modulated only on the bias current of the transmitter laser but not the receiver laser. As the result, even in the back-to-back situation, degradation in the decoded message is unavoidable. With a fiber placed between the transmitter and the receiver lasers, the message recovery of both schemes become worse as that is shown in Figs. 3(b) and (c).

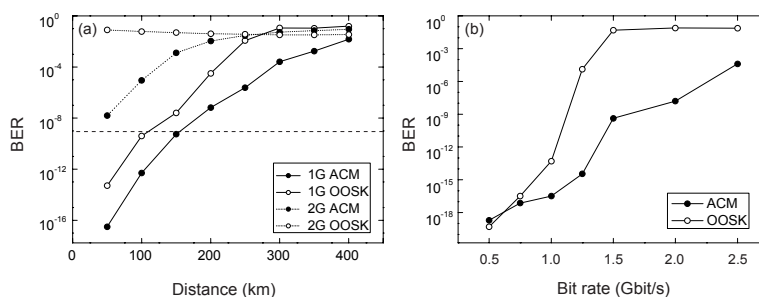


Fig. 4. BER of the ACM and OOSK schemes with different (a) fiber lengths and (b) message bit-rates, respectively. The fiber length in (b) is 50 km.

To quantify the effect of the fiber length and the message bit-rate on the performance of message recovery, Figs. 4(a) and (b) plot the BER of the recovered messages for different fiber lengths and message bit-rates, respectively. As shown in Fig. 4(a), the BER of the ACM scheme is always lower than the OOSK scheme, and a BER lower than  $10^{-9}$  (dashed line), the benchmark set by conventional communications, can be achieved for fiber shorter than 150 km with a 1 Gbps message bit-rate. For higher message bit-rate, the performance of the OOSK scheme is severely degraded compared to the ACM scheme. Fig. 4(b) shows the BER of the ACM and the OOSK schemes with different message bit-rates. As can be seen, while both schemes deteriorate as the bit-rate increases, the ACM scheme clearly outperforms the OOSK scheme except in the case of very low bit-rate. This is because that, in the OOSK scheme, the message is encoded by switching the laser back and forth between two different chaotic states. As the message bit-rate increases and approaches the relaxation oscillation frequency of the laser, the laser does not have sufficient time to stabilize in one state before it is suddenly being switched to the other. Hence, this transient effect makes message recovery more difficult that large synchronization errors are observed in both the ON and the OFF states. Compared to the OOSK scheme, message modulation in the ACM scheme is done within the same chaotic state. Therefore, since the transmitter and the receiver lasers are synchronized at all time, it shows comparable better message recovery quality. Nevertheless, the maximum achievable bit-rate for both schemes are ultimately limited by the relaxation oscillation frequency of the laser (in our case  $f_r = 2.5$  GHz).

Noted that in reality one cannot find two identical lasers that have exactly the same intrinsic parameters. Therefore, to ensure the robustness of this communication system, the performance

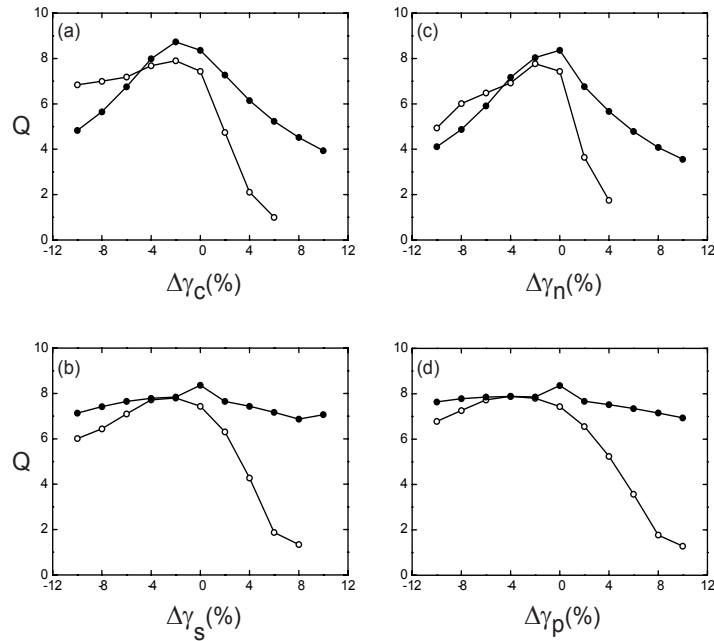


Fig. 5. Message recovery performances of the ACM (solid-circle) and OOSK (opened-circle) schemes for different levels of parameter mismatch with a message bit-rate of 1 Gbps and a fiber length of 50 km. The parameter mismatch between the receiver laser and the transmitter laser is normalized to the parameter of the transmitter laser.

of message recovery for different levels of parameter mismatch between the transmitter and receiver lasers is also studied. Figure 5 shows the message recovery performance of the ACM (solid-circle) and OOSK (opened-circle) schemes for different levels of parameter mismatch with a message bit-rate of 1 Gbps and a fiber length of 50 km. As can be seen, the performance of the ACM scheme is more sensitive to the mismatch in  $\gamma_c$  and  $\gamma_n$ , but not as much in the mismatch in  $\gamma_s$  and  $\gamma_p$ . For the OOSK scheme, the performance with negative parameter mismatch is fairly robust while it drops sharply with positive mismatch. Since the transmitter laser is switched between two different chaotic attractors, the performance (or equivalently, the shape of the curve) of the OOSK scheme is strongly depending on the attractors of the ON and OFF states initially chosen. In any case, the performances of both schemes are shown to be at a level above the benchmark ( $Q=6$ ) in a range of mismatch of around 10 percents, which is considered practical in real applications. More detailed analysis on the robustness of this chaotic communication system will be reported separately.

In sum, the ACM scheme has better performance compared to the OOSK scheme in fiber transmission for the optoelectronic feedback system. Message bit-rate greater than 1 Gbps with transmission length over 100 km is feasible. To further study the performance of this chaotic communication system in an ROF scenario, wireless channel with path loss, AWGN, and multipath effect are considered.



## 4. Radio-over-fiber transmission

### 4.1. Description of the wireless channel

In the ROF configuration, the path loss, AWGN, and multipath effect are considered in the wireless channel. While the path loss can be compensated by amplification, effects of AWGN and multipath contribute randomly to the received signal and which cause severe waveform distortions. A two-path Rayleigh channel model [20] that includes a path with a fixed gain and the others with random path delays and attenuations is considered in this study. The received signal  $s_r$  and the probability density function  $p(r)$  of Rayleigh channel can be expressed by

$$s_r = r \exp[j(\omega_0 t + \theta)] \quad (5)$$

$$p(r) = \begin{cases} \frac{r}{\sigma_r^2} \exp\left(-\frac{r^2}{2\sigma_r^2}\right) & r \geq 0 \\ 0 & \text{otherwise} \end{cases} \quad (6)$$

, where  $r \exp(j\theta) = \sum_{i=1}^n a_i \exp(j\theta_i)$ ,  $\omega_0$  is the angular frequency of signal,  $n$  is the total number of the signals,  $a_i$  and  $\theta_i$  present the amplitude and the phase of the  $i_{th}$  path, and  $\sigma_r^2$  is the Gaussian random variables, respectively. An indoor environment of the wireless channel is assumed that the path delay and attenuation are randomly distributed between 1 to 100 ns and 0 to -20 dB, respectively.

### 4.2. Results with wireless channel

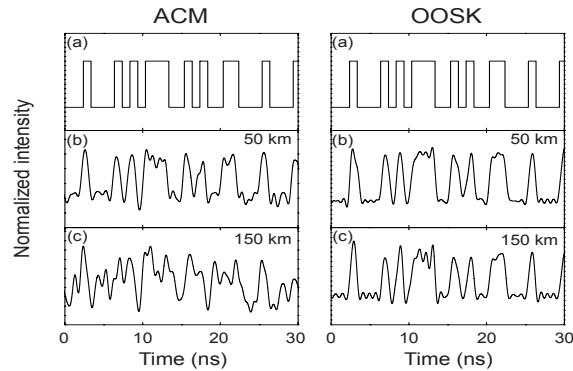


Fig. 6. Decoded messages of the ACM and OOSK schemes in ROF after propagating over wireless channel and fiber with lengths of (a) encoded message for reference, (b) 50 km, and (c) 150 km, respectively.

We consider the path loss, AWGN, and multipath effects in the wireless channel together with the dispersion and nonlinearity effects in the fiber module studied above. Figure 6 shows the encoded and the decoded messages of the ACM and the OOSK schemes for the ROF transmission, where Fig. 6(a) is the encoded message for reference. As can be seen in Figs. 6(b) and (c), when the fiber transmission length increases from 50 km to 150 km, the decoded messages in the ACM scheme distort much more severely than that of the OOSK scheme. To quantify the performance, BER for different transmission distances of the ACM and the OOSK schemes in ROF scenario are shown in Fig. 7.

Figure 7 shows the performance of the chaotic communication system in ROF transmission with different fiber lengths. Since the random effect of the multipath dominates the waveform



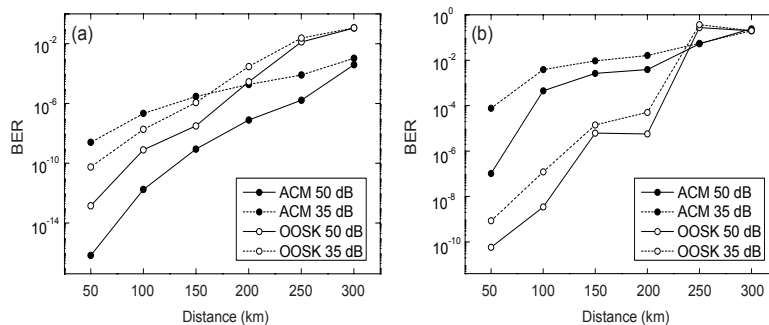


Fig. 7. BER of the ACM and OOSK schemes in ROF with different fiber lengths and message bit-rates, where (a) without and (b) with multipath effect.

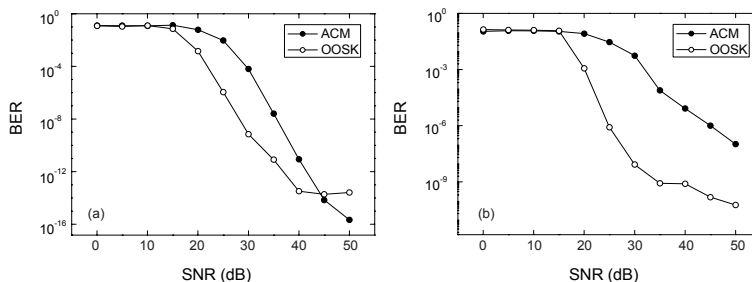


Fig. 8. Performance of the ACM and OOSK schemes in ROF with different SNR for fiber length of 50 km, where (a) without and (b) with multipath effect.

distortion in the wireless channel, we show the performance of both without and with this effect in Figs. 7(a) and (b), respectively. As shown in Fig. 7(a), when the SNR is high enough (50 dB:solid curves), the ACM scheme performs better than the OOSK scheme when only path loss and AWGN are considered in the wireless channel. However, when the SNR is relatively low (35 dB:dashed curves), the synchronization in the ACM scheme is destroyed by the large noise presented in the wireless channel from the amplifier and AWGN noises and hence the performance is comparably worse. When the multipath effect is taken into account as shown in Fig. 7(b), the OOSK outperforms the ACM scheme. With a fiber length of 50 km and an SNR of 50 dB (solid curves in Fig. 7(b)), the BER of the OOSK scheme is as low as  $10^{-10}$  while the ACM scheme has a BER worse than  $10^{-7}$ . This is because the decoding in the ACM scheme requires precise synchronization to recover the encoded message and which becomes very difficult when elevated noise and random effects are presented. On the contrary, it is comparably easy in the OOSK scheme that the decoding is done simply by distinguishing if the transmitter and the receiver lasers are in the same or different states. Figures 8(a) and (b) show the performance of the ACM and the OOSK schemes for different SNR without and with the multipath effect, respectively. As can be seen in Fig. 8(a), while both schemes can achieve a benchmark performance of  $\text{BER} = 10^{-9}$ , the OOSK scheme performs slightly better than the ACM scheme when only the path loss and AWGN noise are included in the wireless channel. When the multipath effect is taken into account, as shown in Fig. 8(b), the OOSK scheme

clearly outperforms the ACM scheme and the benchmark can still be reached for SNR above 35 dB. As the result, the OOSK schemes shows to possess better noise tolerability than the ACM scheme, which is extremely important in a practical communication environment such as the ROF scenario discussed here.

## 5. Conclusion

We have numerically studied the performance of a chaotic communication system with a radio-over-fiber channel based on optoelectronic feedback semiconductor lasers. Two different encoding schemes, namely ACM and OOSK, are investigated and compared. In the fiber transmission module, the dispersion and nonlinearity effects of fiber and the amplified spontaneous emission noise of the amplifiers are considered. The ACM scheme shows better performance than the OOSK for different transmission distances and message bit-rates. In the radio-over-fiber scenario that includes the multipath and AWGN effects in the wireless channel, the OOSK scheme outperforms the ACM scheme that it shows better noise immunity.

This work is supported by the National Science Council of Taiwan under contract NSC 95-2112-M-007-011.